Unisexual reproduction promotes competition for mating partners in the global human fungal pathogen *Cryptococcus deneoformans*

Ci Fu, Torin P. Thielhelm, and Joseph Heitman [1]

1 Department of Molecular Genetics and Microbiology, Duke University Medical Center, Durham, NC, 27710, USA

Corresponding author:

Joseph Heitman, MD, PhD

Department of Molecular Genetics and Microbiology

Duke University Medical Center

322 CARL Building Box 3546

Durham, NC 27710, USA

Tel: 919-684-2824

Fax: 919-684-2790

Email: heitm001@duke.edu

Running title: Foraging for mating in *Cryptococcus deneoformans*

Abstract

Courtship is pivotal for successful mating. However, courtship is challenging for the *Cryptococcus neoformans* species complex, comprised of opportunistic fungal pathogens, as the majority of isolates are α mating type. In the absence of mating partners of the opposite mating type, *C. deneoformans* can undergo unisexual reproduction, during which a yeast-to-hyphal morphological transition occurs. Hyphal growth during unisexual reproduction is a quantitative trait, which reflects a strain's ability to undergo unisexual reproduction. In this study, we determined whether unisexual reproduction confers an ecological benefit by promoting foraging for mating partners. Through competitive mating assays using strains with different abilities to produce hyphae, we showed that unisexual reproduction potential did not enhance competition for mating partners of the same mating type, but when cells of the opposite mating type were present, cells with enhanced hyphal growth were more competitive for mating partners of either the same or opposite mating type. Enhanced mating competition was also observed in a strain with increased hyphal production that lacks the mating repressor gene *GPA3*, which contributes to the pheromone response. Hyphal growth in unisexual strains also enables contact between adjacent colonies and enhances mating efficiency during mating confrontation assays. The pheromone response pathway activation positively correlated with unisexual reproduction hyphal growth during bisexual mating and exogenous pheromone promoted bisexual cell fusion. Despite the benefit in competing for mating partners, unisexual reproduction conferred a fitness cost. Taken together, these findings suggest *C. deneoformans* employs

hyphal growth to facilitate contact between colonies at long distances and utilizes pheromone sensing to enhance mating competition.

Author Summary

Sexual reproduction plays a pivotal role in shaping fungal population structure and diversity in nature. The global human fungal pathogen *Cryptococcus neoformans* species complex evolved distinct sexual cycles: bisexual reproduction between mating partners of the opposite mating types, and unisexual reproduction with only one mating type. During both sexual cycles, cells undergo a yeast-to-hyphal morphological transition and nuclei diploidize through either cell-cell fusion followed by nuclear fusion during bisexual reproduction or endoreplication during unisexual reproduction. Despite the complex sexual life cycle, the majority of Cryptococcal isolates are α mating type. Albeit the scarcity of *MAT***a** cells in the environment, meiotic recombination is prevalent. To decipher this conundrum, we ask whether there is an underlying mechanism in which *Cryptococcus* species increase their mating opportunities. In this study, we showed that the undirected hyphal growth during unisexual reproduction enables *MAT*α cells to forage for mating partners over a larger surface area, and when *MAT*α hyphae come into close proximity of rare *MAT***a** cells, pheromone response pathway activation in both *MAT*α and *MAT***a** cells can further enhance mating. This mating enhancement could promote outcrossing and facilitate genome reshuffling via meiotic recombination.

Introduction

Successful courtship is key to the evolutionary success of sexual organisms, and many species have evolved distinct strategies to locate and choose a mating partner. For example, primates and humans utilize aggression to secure a mating partner [1]; male hummingbirds apply acoustic control using tail feathers during high-speed dives to court females [2]; male *Drosophila* vibrate their wings to generate different songs to trigger mating responses in females [3]; male tree-hole frogs also adopt acoustic strategies taking advantage of tree trunk cavities to attract females [4]; and female pipefish display a temporal striped pattern ornament to woo male partners [5]. These examples demonstrate that complex eukaryotic organisms can employ visual, vocal, or mechanical tactics to secure a mate and transmit their genetic traits to the next generation.

In eukaryotic fungal systems, mating often involves a morphological transition. *Saccharomyces cerevisiae* yeast cells undergo polarized growth and form shmoo projections in preparation for cell fusion during mating [6]. In filamentous fungi, including both ascomycetes and basidiomycetes, sexual reproduction involves the formation of a fruiting body (perithecium or basidium, respectively) [7]. *Candida albicans*, an ascomycete, undergoes a white-opaque switch to initiate mating [8]. Despite their divergent sexual strategies, these morphological transitions are all controlled by the pheromone response pathway [9]. During yeast mating, physical agglutination of yeast cells does not promote courtship, but rather a gradient of pheromone signals is crucial for successful

97 cell-cell fusion during early mating [10, 11]. Similarly, in *Schizosaccharomyces*
98 *pombe*, local pheromone signals and a spatially focal pheromone response
99 dictate cell-cell pairing and fusion position during early mating processes [12, 13].
100 In *C. albicans*, overexpression of the pheromone response MAP kinase pathway
101 components can enhance mating efficiency [14]. These studies establish that the
102 pheromone response pathway plays a critical role in promoting fungal mating
103 efficiency.

104

105 The opportunistic human fungal pathogen *Cryptococcus deneoformans*
106 undergoes a yeast-to-hyphal morphological transition upon mating induction [15].
107 This species has two modes of sexual reproduction: bisexual reproduction
108 between cells of opposite mating types and unisexual reproduction involving cells
109 of only one mating type [15-17]. Cell fusion between *MAT***a** and *MAT*α cells
110 during bisexual reproduction, and between two *MAT*α cells during unisexual
111 reproduction, triggers hyphal development [18]. This morphological transition is
112 orchestrated by the pheromone response pathway [18, 19]. However, recent
113 studies have shown that hyphal growth during unisexual reproduction can also
114 occur independent of cell fusion and the pheromone response pathway [20-23],
115 and that pheromone-independent hyphal development is dependent upon the
116 calcineurin pathway [20, 24].

117

Because the majority of identified natural and clinical *C. neoformans* isolates are of the α mating type, unisexual reproduction likely has significant ecological impacts on the *Cryptococcus* species complex population structure and diversity [25-27]. The limited abundance of *MAT***a** cells in natural environments restricts outcrossing and in the absence of **a**-α mating, unisexual reproduction has been shown to reverse Muller's rachet and offset the low abundance of *MAT***a** cells to avoid an evolutionary dead end [28]. Unisexual reproduction can also generate genotypic and phenotypic diversity *de novo* [29]. Interestingly, population genetics studies have revealed that genome recombination occurs frequently among environmental isolates [30-32], even those that are exclusively α mating type, providing evidence that unisexual reproduction involving fusion of *MAT*α cells of distinct genotypes allows meiotic recombination in nature. Despite these evolutionary benefits, cell fusion-independent solo-unisexual reproduction also occurs and because this pathway involves genetically identical genomes, it does not contribute to genome reshuffling or recombination. Similar to pseudohyphal differentiation in *S. cerevisiae*, *C. deneoformans* hyphal growth during unisexual reproduction has an ecological benefit in promoting foraging for nutrients and habitat exploration in the surrounding environments [33, 34]. In this study, we address whether the ability to undergo unisexual reproduction has an additional ecological benefit in promoting foraging for mating partners to facilitate outcrossing and enable recombination in nature.

Results and Discussion

Strains with enhanced unisexual reproduction potential are more competitive for mating partners of the opposite mating type

During *C. deneoformans* solo-unisexual reproduction, cells undergo the yeast-to-hyphal morphological transition independent of cell fusion and nuclei diploidized through endoreplication [16, 23]. The hyphal growth is a quantitative trait associated with unisexual reproduction that can be used to determine a strain's ability to undergo unisexual reproduction [35]. Although solo-unisexual reproduction occurs independently of cell-cell fusion, cells can fuse with partners of both the same or opposite mating type at varying frequencies [16, 23]. To test whether the ability to undergo unisexual reproduction impacts competition for mating partners during outcrossing, we performed mating competition experiments employing three *MAT*α and three *MAT***a** *C. deneoformans* strains with different degrees of unisexual reproduction potential based on their abilities to produce hyphae (Figure 1A) [35]. Among these strains, several were F2 progeny derived from crosses between the environmental *MAT***a** isolate NIH433 and the clinical *MAT*α isolate NIH12 including a high hyphal (HH) strain XL190α, an intermediate hyphal (MH) strain XL280α, a low hyphal strain XL187**a**, and a no hyphal (NH) strain JEC20**a** [15, 16, 36-38]. LH strain JEC21α and MH strain XL280**a** are congenic strains of JEC20**a** and XL280α, respectively, derived through 10 rounds of backcrossing (Figure S1) [36, 38, 39]. For each mating competition experiment, cells of three strains with different hyphal growth carrying dominant, selectable drug resistance markers were mixed, spot-

164 inoculated, and incubated on V8 agar media for 4 days (Figure 1B). Cells were
165 recovered on YPD medium to obtain colony forming units (CFU), and on YPD
166 medium supplemented with different two-drug combinations to determine the cell
167 fusion frequencies. Cell fusion frequencies were compared between different
168 pairs of strains within the same competition mating mixture to determine whether
169 the ability to undergo unisexual reproduction confers benefits in competition for
170 mating partners to facilitate outcrossing (Figure 1B).

171 Prior to the mating competition experiments, cell fusion frequencies were
172 compared between different hyphal strains. During α-α cell fusion, the *MAT*α MH
173 strain displayed a significantly higher cell fusion frequency (5 cell fusion events
174 per million CFU) compared to the HH and LH strains (0.013 and 0.019 cell fusion
175 events per million CFU, respectively), in which cell fusion rarely occurred (Figure
176 1C). This suggests that the ability to undergo more robust hyphal growth is not
177 strictly correlated with α-α cell fusion efficiency. In contrast, during **a**-α cell fusion,
178 hyphal growth positively correlated with **a**-α cell fusion efficiency. MH-HH strains
179 had a cell fusion frequency (53 cell fusion events per thousand CFU) about 109
180 times higher than LH-MH strains, which in turn had a cell fusion frequency (0.49
181 cell fusion events per thousand CFU) about 26 times higher than NH-LH strains
182 (0.019 cell fusion events per thousand CFU) (Figure 1D). In all of the strains
183 tested, **a**-α cell fusion occurred at a much higher level compared to α-α cell
184 fusion, similar to previous findings [16, 23].

185 Cell fusion has been previously shown to be dispensable for solo-
186 unisexual reproduction [19, 23], which can account for the observed poor

187 correlation between hyphal growth and α-α cell fusion frequency. Thus, we
188 hypothesize that increased hyphal growth may not provide an advantage in
189 competing for mating partners of the same mating type. Indeed, when we
190 performed the unisexual mating competition assay mixing the HH, MH, and LH
191 cells, we observed that HH and LH cells yielded the most fusion products with a
192 cell fusion frequency of 1.3 cell fusion events per million CFU that is not
193 significantly different from cell fusion frequencies involved MH cells (Figure 1E)
194 that exhibited the highest cell fusion frequency (Figure 1C). These findings
195 indicate that neither α-α cell fusion frequency nor hyphal growth can be used to
196 predict mating partner preference during unisexual reproduction, which supports
197 the hypothesis that the ability to undergo unisexual reproduction does not
198 promote competition for mating partners of the same mating type.

199 To test whether the propensity for unisexual reproduction plays a role in
200 competing for mating partners of the opposite mating type, mating competition
201 assays were conducted for a given *MAT***a** isolate between two *MAT*α strains of
202 different hyphal growth phenotypes (Figure 2A). Interestingly, cells capable of
203 producing more hyphae always had a significantly higher cell fusion frequency
204 with *MAT***a** cells compared to cells with lower hyphal growth potential (Figure 2A,
205 Table S1). For example, in the presence of MH *MAT***a** cells, HH *MAT*α cells fused
206 with *MAT***a** cells 24 times more efficiently than LH *MAT*α cells and 8.1 times more
207 efficiently than MH *MAT*α cells, and MH *MAT*α cells fused with *MAT***a** cells 5.8
208 times more efficiently than LH *MAT*α cells (Table S1). These results suggest that
209 increased hyphal growth correlates with competition for mating partners of the

opposite mating type during bisexual reproduction. It was also noted that the mating competition advantage decreased for each competition pair (24, 14.5, and 8.9 fold differences for HH vs LH, 8.1, 6.5, and 5.3 fold differences for HH vs MH, and 5.8, 4.6, and 1.7 fold differences for MH vs LH) with the decreasing hyphal phenotype of the *MAT***a** cells (Figure 2A and Table S1), suggesting that increased hyphal growth of *MAT***a** cells can also promote cell fusion.

Besides the observation that hyphal growth enhanced competition for mating partners of the opposite mating type, the presence of higher hyphal *MAT*α cells also stimulated **a**-α cell fusion. MH *MAT***a** and HH *MAT*α cells fused at a frequency of 52 cell fusion events per thousand CFU in the presence of MH *MAT*α cells compared to 10 cell fusion events per thousand CFU in the presence of LH *MAT*α cells (5.2-fold) (Dark yellow-shaded cells in Table S1). MH *MAT***a** and MH *MAT*α cells fused at a frequency of 6.4 cell fusion events per thousand CFU in the presence of HH *MAT*α cells compared to 3.4 cell fusion events per thousand CFU in the presence of LH *MAT*α cells (1.9-fold) (Dark blue-shaded cells in Table S1). Similar trends were observed during competition for LH *MAT***a** cells in that the presence of MH *MAT*α cells increased LH *MAT***a** and HH *MAT*α cell fusion frequency by 4.5-fold compared to the presence of LH *MAT*α cells (Medium yellow-shaded cells in Table S1), and the presence of HH *MAT*α cells increased LH *MAT***a** and MH *MAT*α cell fusion frequency by 2.2-fold compared to the presence of LH *MAT*α cells (Medium blue-shaded cells in Table S1). However, cell fusion frequencies between *MAT***a** cells and LH *MAT*α cells were comparable in the presence of HH or MH *MAT*α cells (0.41 or 0.59 cell fusion

233 events per thousand CFU for MH *MAT***a** cells, and 0.02 or 0.02 cell fusion events
234 per thousand CFU for LH *MAT***a** cells) (Dark and medium green-shaded cells in
235 Table S1). Interestingly, no enhancement of cell fusion frequency by high hyphal
236 *MAT*α cells was observed during competition for NH *MAT***a** cells (light color-
237 shaded cells in Table S1). Notably, the enhancement of cell fusion frequency by
238 higher hyphal *MAT*α cells did not occur when either *MAT***a** NH or *MAT*α LH cells
239 were involved in **a**-α cell fusion, suggesting that strains with poor unisexual
240 reproduction potential have a disadvantage in competing for mating partners of
241 the opposite mating type.

242

243 The ability to undergo unisexual reproduction also correlated with cell
244 fusion between cells of the same mating type when a *MAT***a** partner is present. In
245 the presence of MH or LH *MAT***a** cells, HH and MH *MAT*α cells fused at higher
246 frequencies (26 and 27 cell fusion events per million CFU, respectively)
247 compared to HH and LH *MAT*α cells (8.1 and 3.4 cell fusion events per million
248 CFU, respectively), and in the presence of MH, or LH, or NH *MAT***a** cells, HH and
249 LH *MAT*α cells fused at higher frequencies (8.1, 3.4, and 2.8 cell fusion events
250 per million CFU, respectively) compared to MH and LH *MAT*α cells (0.71, 0.28,
251 and 0.14 cell fusion events per million CFU, respectively) (Figure 2B), suggesting
252 that increased hyphal growth correlated with enhanced α-α cell fusion frequency
253 in the presence of *MAT***a** cells. We also observed a trend where α-α cell fusion
254 frequencies (HH and MH, HH and LH, and MH and LH) decreased with reduced
255 hyphal *MAT***a** cells (Figure 2B), suggesting that the presence of more robust

hyphal *MAT***a** cells can further enhance α-α cell fusion. In summary, strains with robust hyphal production have an advantage in competing for mating partners of the opposite mating type, and also for mating partners of the same mating type when cells of the opposite mating type are present.

*gpa3*Δ mutation enhances competition for mating partners of the same or opposite mating type

The pheromone response pathway plays an important role in the yeast-to-hyphal morphological transition during *C. deneoformans* sexual reproduction. This signaling cascade is controlled by G proteins and RGS proteins, including the Gα protein Gpa3 which represses hyphal growth during mating [40-43]. To further examine the impact of the ability to undergo unisexual reproduction during mating competition, we generated strains enhanced for hyphal production by deleting the *GPA3* gene in the LH strain JEC21α. *gpa3*Δ mutants exhibited significantly increased hyphal growth during both unisexual and bisexual reproduction compared to the parental strain (Figure 3A). Next, mating competition assays were conducted using the enhanced hyphal (EH) strain JEC21α *gpa3*Δ to test its ability to compete for mating partners.

Similar to the observation in HH, MH, and LH strains, enhanced hyphal production did not increase cell fusion between *MAT*α cells but did increase cell fusion frequency by 4-fold between *MAT***a** and *MAT*α cells compared to the

parental LH strain (Figure 3B, C). However, the increase is not statistically significant due to the low cell fusion frequencies between strains of low hyphal background. Unisexual mating competition assays were performed to compare the abilities of LH and EH *MAT*α cells to fuse with MH *MAT*α cells. In the control assay, cell fusion frequencies were comparable between cells of all three strain combinations (MH with LH-*NAT*, MH with LH-*NEO*, and LH-*NAT* with LH-*NEO*) (Figure 3D). In the assay mixing LH, MH, and EH cells, EH cells fused with MH cells at a significantly higher frequency of 2.8 cell fusion events per million CFU compared to LH cells (85-fold) (Figure 3E), suggesting that deletion of *GPA3* increases competitiveness for mating partners of the same mating type. In the mating competition during bisexual reproduction, no advantage was observed in the fusion of NH *MAT***a** cells with either EH or the parental LH *MAT*α cells (Figure 3G). However, a significant 2.9-fold increase was observed in total **a**-α cell fusion events during mating competitions for NH *MAT***a** cells between EH and LH *MAT*α cells compared to control mating competitions for the same *MAT***a** cells between LH-*NAT* and LH-*NEO MAT*α cells (Figure 3F-3G), indicating that presence of cells with enhanced ability to undergo unisexual reproduction allows both EH and LH *MAT*α cells to fuse with *MAT***a** mating partners more efficiently during bisexual reproduction. A significant 2.9-fold increase was observed in α-α cell fusion between EH and LH *MAT*α cells in the presence of NH *MAT***a** cells compared to cell fusion between LH-*NAT* and LH-*NEO MAT*α cells (Figure 3H), suggesting that in the presence of *MAT***a** cells, *GPA3* deletion also enhances competition for mating partners of the same mating type. Overall, this analysis of

the enhanced hyphal growth strain JEC21α *gpa3*Δ provides additional support for models in which increased unisexual reproduction potential enhances competition for mating partners.

Hyphal growth promotes foraging for mating partners

Unisexual reproduction provides evolutionary and ecological benefits for *C. deneoformans* by generating aneuploid progeny with phenotypic diversity and by promoting habitat exploration through hyphal growth [29, 34]. Here we further show that unisexual cells have an advantage in competing for mating partners within the same colony. We tested whether hyphal growth during unisexual reproduction confers benefits in foraging for mating partners.

Both long-term and short-term foraging for mating partner experiments suggested that hyphal growth promoted foraging for mating. In a six-week mating confrontation experiment, hyphae of different *MAT*α unisexual reproduction backgrounds marked with NEO grew towards the same *MAT***a** cells marked with HYG that were 4 mm apart (Figure 4A, B). When competing for either the same *MAT***a** or *MAT*α cells (except LH *MAT*α cells), although not all pairwise comparisons by t-test were significant due to the lack of contact when strains of no or low hyphal growth were involved, a significant trend by one-way ANOVA was observed that isolates with more hyphal growth yielded more double drug resistant colonies than isolates with reduced hyphal growth (Figure 4C and Table S2). In a seven-day mini-colony mating experiment, colonies derived from single

323 cells produced hyphae that allowed contact with adjacent colonies of the
324 opposite mating type (Figure S2A). Similar to the long-term mating confrontation
325 experiment, a significant trend by one-way ANOVA was observed in which
326 isolates with more hyphal growth had an advantage in forming double drug
327 resistant colonies (Figure S2B and Table S3). Although pairwise comparisons by
328 t-test showed significant differences between crosses involved NH and LH cells
329 that were not observed in the confrontation experiment, this discrepancy is due to
330 differences in the experimental setup where cells were inoculated at 0.4 cm apart
331 during confrontation, whereas randomly plated on agar media during mini-colony
332 mating experiment, where colony contact is enabled by both hyphal growth and
333 chance. Overall, these results suggest that hyphal growth during unisexual
334 reproduction can facilitate contact between mating partners in adjacent
335 environments.

336

337 **Pheromone response pathway activation is correlated with hyphal growth**
338 **phenotype during bisexual reproduction**

339 Elevated pheromone response pathway activation and increased
340 response to pheromones are critical to successful courtship during mating in *S.*
341 *cerevisiae* and *C. albicans* [10, 11, 14]. *S. cerevisiae* utilizes the α-factor
342 protease Bar1 and **a**-factor barrier Afb1 to discriminate mating partners with
343 different pheromone levels and drive evolution towards higher pheromone
344 production for efficient mating [44-47]. Pheromones also stimulate mating and
345 the yeast-to-hyphal morphological transition during *C. neoformans* bisexual

346 reproduction [48]. To determine the role of the pheromone response pathway
347 during *C. deneoformans* mating competition, expression levels were examined
348 for the genes encoding the pheromones MFα and MF**a**, the pheromone receptors
349 Ste3α and Ste3**a**, the MAP kinase Cpk1, the transcription factors Mat2 and Znf2,
350 and the plasma membrane fusion protein Prm1 [23, 40, 49].

351 Pheromone response pathway activation did not correlate with the hyphal
352 growth phenotype in *MAT***a** or *MAT*α strains. In *MAT***a** strains, all of the
353 pheromone response pathway genes were significantly upregulated in the MH
354 strain XL280**a** compared to the LH and NH strains, but only *MF***a** and *PRM1* were
355 significantly upregulated in the LH strain XL187**a** compared to the NH strain
356 JEC20**a** (Figure S3). In *MAT*α strains, all of the pheromone response pathway
357 genes were significantly upregulated in the HH and MH strains compared to the
358 LH strain JEC21α, but the MH strain XL280α had a significantly higher
359 pheromone pathway activation compared to the HH strain XL190α (Figure S3).
360 The pheromone pathway was significantly upregulated in the EH strain JEC21α
361 *gpa3*Δ compared to the parental LH strain JEC21α (Figure S3). These
362 expression analyses suggest that pheromone response pathway activation *per*
363 *se* is not sufficient to explain the ability to undergo unisexual reproduction and its
364 association with competition for mating partners. It was previously shown that the
365 cell fusion protein Prm1 is not required for unisexual reproduction [23], and
366 certain environmental factors, such as copper and glucosamine, can induce
367 hyphal growth independently of the pheromone response pathway [20, 21]. In a
368 recent study on the quorum sensing peptide Qsp1, deletion of pheromone and

pheromone receptor genes had little impact on hyphal growth during unisexual reproduction [22], further indicating the polygenic nature of unisexual reproduction.

Despite the incongruent association of the pheromone response pathway and the ability to undergo unisexual reproduction, pheromone response pathway activation was positively correlated with the hyphal growth during bisexual reproduction. The α pheromone gene *MF*α, both **a** and α pheromone receptor genes *STE3*α and *STE3***a**, and the plasma membrane fusion gene *PRM1* showed significant correlation with the hyphal growth phenotype (Figure 5A). Although *MF***a** expression was lower in the cross between **a** MH and α HH strains compared to **a** LH and α MH strains, the significant upregulation of the *MF*α, *STE3*α, and *STE3***a** may compensate for the overall pheromone response activation (Figure 5A). The gene expression patterns of two transcription factors Mat2 and Znf2 that regulate yeast-to-hyphal morphological transition and mating significantly correlated with the hyphal growth except for the cross between **a** MH and α HH strains. Nonetheless, these two genes were expressed at higher levels compared to the cross between **a** LH and α MH strains (Figure 5A). The expression of the MAP Kinase *CPK1* gene poorly correlated with hyphal growth (Figure 5A), which is likely due to post-translational control of the MAP kinase through phosphorylation, which can relieve a requirement for expression level upregulation during pathway activation. Overall, the pheromone response pathway activation is largely congruent with the hyphal growth phenotype suggesting that in the presence of cells of the opposite mating type, unisexual

392 cells are capable of upregulating the pheromone response pathway in both
393 *MAT***a** and *MAT*α cells to compete for mating partners.

394 To validate that pheromone contributes to mating competitiveness, we
395 tested whether synthetic α pheromone promotes **a**-α cell fusion. Indeed,
396 exogenous α pheromone promoted cell fusion between **a** NH and α LH cells in a
397 dose dependent manner (Figure 5B). However, the enhancement of cell fusion
398 frequency by pheromone is limited, compared to the 2788-fold increase of cell
399 fusion frequency between **a** MH and α HH cells over **a** NH and α LH cells (Figure
400 1D) that coincided with a 34.5-fold increase in α pheromone expression (Figure
401 5A). Interestingly, the mild increase in cell fusion by exogenous pheromone is not
402 observed in the cross between **a** NH and α EH cells (Figure S4A), which is likely
403 due to the saturation of Ste3**a** by the 1184-fold higher α pheromone expressed
404 by α EH cells (Figure S3). The less than two-fold increase in cell fusion provided
405 by 5 μM exogenous pheromone suggested that changes in α pheromone alone
406 are not able to tip the balance and drive the entire pheromone response pathway
407 towards a stronger increase in mating efficiency. In support, exogenous supply of
408 500 nM pheromone provided limited impact in cell fusion between cells of higher
409 hyphal growth phenotypes (Figure S4A); and when hyphal growth was
410 suppressed under nutrient rich conditions, exogenous pheromone had little to no
411 impact on cell fusion (Figure S4B).

412 In response to the pheromone signal, *S. cerevisiae* undergoes filamentous
413 growth to enhance the probabilities of cells finding a mating partner [50]. Here we
414 observed that the **a** EH colonies responded to 5 μM α pheromone peptide and

415 produced abundant hyphae (Figure 5C), similar to previous report [51],
416 suggesting that pheromone can promote hyphal growth and increase the contact
417 opportunities between adjacent colonies within the same environment.

418

419 **_gpa3_Δ mutation resulted in a fitness cost**

420 Upregulation of the pheromone response pathway enhances mating
421 efficiency; however, this upregulation can result in a fitness cost in *S. cerevisiae*
422 and *C. albicans* [14, 52]. In yeast, a short-term experimental evolution
423 experiment showed that mutations abrogating expression of 23 genes involved in
424 mating conferred a fitness benefit during yeast growth when functions of these
425 genes are not required [52]. In *C. albicans*, cells undergo a white-opaque switch
426 and upregulate the pheromone response pathway, which results in a fitness cost
427 for the opaque cells [14]. Given that the pheromone response pathway is
428 activated at a higher level in *C. deneoformans* strains with more hyphal growth
429 during bisexual reproduction (Figure 5A), we investigated whether unisexual
430 reproduction confers a fitness cost.

431 Growth curve analyses in YPD liquid medium were performed using an
432 automated Tecan Sunrise absorbance reader to determine the fitness of different
433 strains. The cultures were agitated with vigorous shaking for one minute bihourly
434 before each OD_{600} measurement. The minimum agitation allows for
435 differentiation of growth curve kinetics among the strains tested, which would
436 otherwise be indistinguishable when grown on solid YPD medium. Compared to

437 the low hyphal growth strains JEC21α and JEC20**a**, *gpa3*Δ mutants exhibited a
438 growth defect in nutrient rich media, suggesting that deletion of *GPA3* resulted in
439 a fitness cost (Figure S5). However, this fitness cost was not due to the yeast-to-
440 hyphal morphological transition as hyphal growth was not present. Interestingly,
441 deletion of the *GPA3* gene in the sister species *C. neoformans* did not induce
442 hyphal growth or cause a growth defect compared to the non-hyphal strain
443 KN99**a** (Figure S5). It has been shown that the pheromone response pathway
444 activation by *GPA3* gene deletion is lower in KN99**a** than in JEC21 or JEC20,
445 indicating that deletion of *GPA3* is not sufficient to rewire cellular responses to
446 induce unisexual reproduction in *C. neoformans* [40].

447 We next performed fitness competition experiments. After 10 days of
448 incubation of equally mixed cells on YPD and V8 agar medium, cells were
449 collected and plated on selection media to determine colony forming units for
450 each competition strain. Hyphal growth was observed on both YPD and V8
451 media when **a** MH cells were present, and both yeast cells and hyphae were
452 collected to compare fitness (Figure S6). During competition between two LH
453 strains, cells were recovered at about 1 to 1 ratio after 10-day incubation on both
454 YPD and V8 media both in the absence or in the presence of **a** cells (Figure 6A).
455 In contrast, LH strain outcompeted EH strain when cells were incubated on V8
456 medium or when **a** cells were present (Figure 6B). On YPD medium in the
457 absence of **a** cells, the EH strain that displayed poor growth in liquid media
458 (Figure S5) outcompeted the parental LH strain(Figure 6B), which is likely due to
459 differential cellular responses under different growth conditions. However, this

competition advantage was reversed when **a** cells were present or when mixed cells were incubated on V8 medium (Figure 6B), suggesting that the presence cells of the opposite mating type or the mating inducing environment can elicit a fitness cost. This competition disadvantage for the EH strain on V8 medium was further exacerbated when **a** cells were present during competition (Figure 6B). These fitness competition assays demonstrate that *gpa3*Δ mutation enhances mating competition at a cost of growth fitness, and this fitness cost is likely due to the energy required in the expression of the pheromone response pathway genes. It has been reported that long-term passage on rich media in the lab often diminishes the hyphal growth phenotype of *MAT***a** strains, which further suggests that there is a fitness cost associated with the ability to undergo unisexual reproduction [53]. Interestingly, in *S. cerevisiae*, the [*SWI*$^{+}$] prion state promotes outcrossing efficiency due to a defect in *HO* expression and mating type switching, which also leads to a fitness cost [54]. Taken together, fungal species have evolved different strategies in promoting mating in nature accompanied with a fitness tradeoff.

Conclusion

Sexual reproduction plays a pivotal role in shaping fungal population structure and diversity in nature. However, studies on how fungi secure a mating partner in nature for successful mating are limited. In this study, we aimed to characterize the ecological and evolutionary benefits of unisexual reproduction in *C. deneoformans*. Similar to the landmark study by Jackson and Hartwell showing that higher pheromone production promotes courtship in *S. cerevisiae* [11], we showed that strains with higher potential for unisexual reproduction are more competitive for mating partners of both the same and the opposite mating types when cells of the opposite mating type are present, and the pheromone response pathway activation is positively correlated with the hyphal growth phenotype (Figure 7). More interestingly, in addition to pheromone sensing, unisexual cells employ hyphal growth to increase contact opportunities between colonies at relatively long distances. However, this mating competition advantage results in a fitness cost for unisexual cells during mitotic growth under mating-inducing conditions.

The strains involved in this study were all derived from natural and clinical isolates under laboratory conditions, suggesting that the ability to undergo unisexual reproduction is likely to span a broad range in the environment. The majority of natural and clinical isolates of the *Cryptococcus* species complex are found to be of the α mating type, which accounts for 99% of *C. neoformans* isolates [25-27]. In a survey of *C. deneoformans* environmental distribution around the Mediterranean basin, 27% of isolates are *MAT***a** isolates, which were

all recovered in Greece, suggesting certain environmental niches harbor *MAT***a** cells [27]. Genomic and genetic evidence also suggest that recombination is prevalent among these environmental isolates, and some isolates are isolated from a single *Eucalytus* hollow, which underscores that mating occurs in nature [30-32]. Although sexual structures of *Cryptococcus* species have yet to be documented in nature, plant material-based media such as V8, on which we conducted the mating competition assays, can readily induce sexual reproduction under laboratory conditions, suggesting that the mating competition we observed could happen in its environmental niche. We hypothesize that in the presence of *MAT***a** cells sparsely distributed in the environment, undirected hyphal growth first enables unisexual *MAT*α cells to forage for mating partners over a much larger surface area than is available to cells within a much more compact budding yeast colony. Next, as *MAT*α hyphae come into the proximity of rare *MAT***a** cells, pheromone response pathway activation in both *MAT*α and *MAT***a** cells can further enhance mating competition. This mating competition advantage could promote outcrossing and provide an evolutionary advantage by facilitating genome reshuffling via meiotic recombination in a pathogenic yeast species.

Materials and methods

Strains, media, and growth conditions

Strains used in this study are listed in Table S4. Strains with different hyphal growth phenotypes, XL190α, XL280α, JEC21α, XL280**a**, XL187**a**, and JEC20**a**, were selected to represent high, intermediate, and low hyphal strains [16, 35, 38, 39]. Yeast cells were grown at 30°C on Yeast extract Peptone Dextrose (YPD) medium. Strains harboring dominant selectable markers were grown on YPD medium supplemented with 100 μg/mL nourseothricin (NAT), 200 μg/mL G418 (NEO), or 200 μg/mL hygromycin (HYG) for selection. Mating assays were performed on 5% V8 juice agar medium (pH = 7.0) or Murashige and Skoog (MS) medium minus sucrose (Sigma-Aldrich) in the dark at room temperature for the designated time period.

Drug-resistant marker strain generation and gene deletion

NAT (pAI3) or G418/NEO (pJAF1) resistant expression constructs were introduced into XL190α, XL280α, and JEC21α, and a HYG (pJAF15) resistant expression construct was introduced into XL280α, XL280**a**, XL187**a**, and JEC20**a** ectopically via biolistic transformation as previously described [55-57].

To generate deletion mutants for *GPA3*, a deletion construct consisting of the 5' upstream and 3' downstream regions of *GPA3* gene flanking the *NEO* cassette was generated by overlap PCR as previously described [58]. The *GPA3* deletion construct was introduced into the strain JEC21α via biolistic

transformation. Transformants were selected on YPD medium supplemented with G418, and gene replacement by homologous recombination was confirmed by PCR. Primers used to generate these deletion constructs are listed in Table S5.

Microscopy

Cells were grown on V8 agar medium for seven days or three weeks in the dark at room temperature to allow hyphal formation. Hyphal growth on the edge of mating patches was imaged using a Nikon Eclipse E400 microscope equipped with a Nikon DXM1200F camera.

Competitive mating assays

For each competitive mating assay, cells were grown overnight in YPD liquid medium at 30°C and adjusted to OD_{600}=0.5 in sterile H_2O, and then equal volumes of cells marked with different dominant drug resistant markers were mixed and spot inoculated (50 µl) on V8 agar medium. The mating plates were incubated for four days in the dark at room temperature. The cells were harvested and plated in serial dilution on YPD medium and YPD medium supplemented with different two drug combinations (NAT and NEO, NAT and HYG, or NEO and HYG). The cells were incubated for three to five days at room temperature and colony forming units were counted. Cell fusion frequencies were determined as double drug resistant CFU/total CFU. The complete competitive

mating experimental design is listed in Table S6. Each mating competition was performed in biological triplicate.

Foraging for mating assays

To investigate whether hyphal growth enables cells foraging for mating partners, we performed long-term confrontation and short-term mini-colony mating experiments. For the confrontation mating experiment, HYG resistant XL280**a**, XL187**a**, and JEC20**a** were streaked and grown on V8 medium to form a line of cells, and then NEO resistant XL190α, XL280α, and JEC21α, and JEC21α *gpa3*Δ::*NEO* were spot inoculated 4 mm apart in parallel along the *MAT***a** cells. Unisexual hyphae grew towards cells of the opposite mating type for six weeks. Then the cells were collected and plated on YPD medium supplemented with HYG and NEO. After incubation at room temperature for three to five days, total double drug resistant colony forming units were counted to determine whether hyphal growth conferred an advantage in foraging for mating partners. Each confrontation mating experiment was performed in biological quintuplicate. For the mini-colony mating experiment, the aforementioned HYG resistant *MAT***a** strains and NEO resistant *MAT*α strains were grown overnight in YPD liquid medium and adjusted to OD_{600}=0.008. For each mating pair, 100 µl of *MAT***a** cells and 100 µl of *MAT*α cells were mixed and plated on V8 agar medium to form evenly spaced mini colonies. Unisexual hyphae facilitate contact between adjacent colonies after growing for seven days. Then the cells were collected and plated on YPD medium and YPD medium supplemented with HYG and NEO.

583 The cells were incubated for three to five days at room temperature and colony
584 forming units were counted. Cell fusion frequencies were determined as double
585 drug resistant CFU/total CFU. Each mating was performed in biological triplicate.

586

587 **RNA extraction and qRT-PCR**

588 To examine pheromone response pathway activation, qRT PCR
589 experiments were performed on RNA extracted from cells incubated on V8 agar
590 medium for 36 hours as previously described [23]. In brief, XL190α, XL280α,
591 JEC21α, JEC21α *gpa3*Δ::*NEO*, XL280**a**, XL187**a**, and JEC20**a** were grown
592 overnight in YPD liquid medium and adjusted to OD_{600}=2 in sterile H_2O. Then
593 cells of individual strains and an equal-volume mixtures of cells for crosses
594 between XL190α and XL280**a**, XL280α and XL187**a**, JEC21α and JEC20**a**, and
595 JEC21α *gpa3*Δ::*NEO* and JEC20**a** were spotted (250 µl) on V8 medium and
596 incubated for 36 hours. Cell patches of individual strains and of mixture of **a** and
597 α strains were scraped off the medium and transferred into Eppendorf tubes then
598 flash frozen in liquid nitrogen. RNA was extracted using TRIzol reagent (Thermo)
599 following the manufacturer's instructions. RNA was treated with Turbo DNAse
600 (Ambion), and single-stranded cDNA was synthesized by AffinityScript RT-
601 RNAse (Stratagene). cDNA synthesized without the RT/RNAse block enzyme
602 mixture was used to control for genomic DNA contamination. The relative
603 expression levels of targeted genes were measured by qRT PCR using Brilliant
604 III ultra-fast SYBR green QPCR mix (Stratagene) in an Applied Biosystems 7500
605 Real-Time PCR system. A "no template control" was used to analyze the

606 resulting melting curves to exclude primer artifacts for each target gene. Gene
607 expression levels were normalized to the endogenous reference gene *GPD1*
608 using the comparative ΔΔCt method. Primers used for qRT-PCR are listed in
609 Table S5. For each target gene and each sample, technical triplicate and
610 biological triplicate were performed.

611

612 **Mating assays with exogenous α pheromone peptide**

613 To address whether pheromone promotes mating competition and hyphal
614 growth, carboxyl farnesylated and methylated α pheromone peptide
615 (QEAHPGGMTLC) (synthesized at GenScript, USA) was tested for its impact on
616 mating and hyphal growth. α pheromone peptide was dissolved in methanol at
617 the concentration of 50 μM and 10-fold serial dilutions in methanol were prepared
618 as stock solutions. For the mating assay, *HYG* marked *MAT***a** and *NEO* marked
619 *MAT*α cells were prepared and mixed as mentioned above for the mating
620 competition assays. α pheromone peptide was added to mixed **a** NH (CF926)
621 and α LH (CF759) cells at the concentrations of 0, 500 pM, 5 nM, 50 nM, 500 nM,
622 and 5 μM, and the mixed cells were spot-inoculated on the V8 media and
623 incubated in the dark at room temperature for four days. Cells were then
624 harvested and plated on both YPD and YPD media supplemented with NEO and
625 HYG to determine cell fusion frequency. Same mating assays were carried out
626 for crosses between **a** MH (CF978) and α HH (CF914), **a** LH (CF931) and α MH
627 (CF752), **a** NH (CF926) and α LH (CF759), and **a** NH (CF926) and α EH

(CF1314) both in the absence and in the presence of 500 nM α pheromone peptide on both YPD and V8 media.

To test the impact of α pheromone peptide on hyphal growth, 5 μM α pheromone peptide and methanol were dropped onto MS media and allowed to dry. **a** EH (YPH86) cells were grown overnight and washed with H_2O twice, and then inoculated onto the MS plate with dried α pheromone peptide and methanol droplets at a different spot. Cells were then microscopically manipulated and transferred to the α pheromone peptide and methanol spots. Colony hyphal growth was monitored daily and imaged after incubation in the dark at room temperature for 72 hours.

Fitness competition and growth curve assays

Competition experiments were performed to compare fitness between two low hyphal strains and between low and enhanced hyphal strains both in the absence and in the presence of the **a** MH cells. Overnight cultures of JEC21α *NAT*, JEC21α *NEO*, JEC21α *gpa3*Δ::*NEO*, and XL280**a** were washed with H_2O twice and cell densities were determined with a hemocytometer. For each competition experiment, 10 μl of H_2O containing 100,000 cells of each strain was spotted on either YPD or V8 agar medium and incubated in the dark at room temperature for 10 days. Cells were collected and plated on YPD medium supplemented with NAT or G418 to determine colony forming units. Cell mixtures were plated before incubation to control for equal mixing. Each competition was

650 performed in triplicate. Fitness was determined by calculating the percentile of
651 the recovered CFU of each strain out of the total recovered dominant drug
652 resistant CFU.

653 To determine the growth fitness of different unisexual strains, KN99**a**,
654 KN99**a** *gpa3*Δ::*NEO*, JEC20**a**, JEC20**a** *gpa3*Δ::*NEO*, JEC21α, and JEC21α
655 *gpa3*Δ::*NEO* were grown overnight in YPD liquid medium and washed twice in
656 H_2O. 10,000 cells for each strain were resuspended in 200 µl YPD liquid medium
657 and incubated in a 96-well plate (Corning) at 30°C with vigorous shaking for 1
658 min bihourly. OD_{600} readings were measured bi-hourly after shaking using an
659 automated Tecan Sunrise absorbance reader. Each sample was tested in
660 quintuplicate.

661

662 **Statistical analysis**

663 All statistical analyses were performed using the Graphpad Prism 7
664 program. Welch's t-test was performed for each pairwise comparison, and one-
665 way ANOVA was performed for each group analysis with a *p* value lower than
666 0.05 considered statistically significant (* indicates $0.01<p\leq0.05$, ** indicates
667 $0.001<p\leq0.01$, *** indicates $0.0001<p\leq0.001$, and **** indicates $p\leq0.0001$).

668 **Acknowledgements**

669 We thank Shelby Priest, Daniel Lew, Sheng Sun, and Zanetta Chang for
670 critical reading of the manuscript. This work was supported by NIH/NIAID R37
671 grant AI39115-21 and R01 grant AI50113-15 to J.H.

672

673 **Author Contributions**

674 Conceptualization, C.F., T.P.T., and J.H.; Formal analysis, C.F., T.P.T.,
675 and J.H.; Funding acquisition, J.H.; Investigation, C.F. and T.P.T.; Methodology,
676 C.F., T.P.T., and J.H.; Resources, C.F. and J.H.; Supervision, J.H.; Writing –
677 original draft, C.F.; Writing – review & editing, C.F., T.P.T., and J.H.

678

Declaration of Interests

The authors declare no competing interests.

682 ## References

683

684 1. Muller, M.N., and Wrangham, R.W. (2009). Sexual coercion in primates and humans: an
685 evolutionary perspective on male aggression against females, (Cambridge, Mass.:
686 Harvard University Press).
687 2. Clark, C.J., and Mistick, E.A. (2018). Strategic acoustic control of a hummingbird
688 courtship dive. Curr Biol *28*, 1257-1264.
689 3. Clemens, J., Coen, P., Roemschied, F.A., Pereira, T.D., Mazumder, D., Aldarondo, D.E.,
690 Pacheco, D.A., and Murthy, M. (2018). Discovery of a new song mode in *Drosophila*
691 reveals hidden structure in the sensory and neural drivers of behavior. Curr Biol *28*,
692 2400-2412 e2406.
693 4. Lardner, B., and bin Lakim, M. (2002). Animal communication: tree-hole frogs exploit
694 resonance effects. Nature *420*, 475.
695 5. Berglund, A., and Rosenqvist, G. (2001). Male pipefish prefer ornamented females. Anim
696 Behav *61*, 345-350.
697 6. Ydenberg, C.A., and Rose, M.D. (2008). Yeast mating: a model system for studying cell
698 and nuclear fusion. Methods Mol. Biol. *475*, 3-20.
699 7. Dyer, P.S., Ingram, D.S., and Johnstone, K. (1992). The control of sexual morphogenesis
700 in the ascomycotina. Biol Rev *67*, 421-458.
701 8. Miller, M.G., and Johnson, A.D. (2002). White-opaque switching in *Candida albicans* is
702 controlled by mating-type locus homeodomain proteins and allows efficient mating. Cell
703 *110*, 293-302.
704 9. Jones, S.K., Jr., and Bennett, R.J. (2011). Fungal mating pheromones: choreographing the
705 dating game. Fungal Genet. Biol. *48*, 668-676.
706 10. Jackson, C.L., and Hartwell, L.H. (1990). Courtship in *Saccharomyces cerevisiae*: an early
707 cell-cell interaction during mating. Mol. Cell Biol. *10*, 2202-2213.
708 11. Jackson, C.L., and Hartwell, L.H. (1990). Courtship in *S. cerevisiae*: both cell types choose
709 mating partners by responding to the strongest pheromone signal. Cell *63*, 1039-1051.
710 12. Dudin, O., Merlini, L., and Martin, S.G. (2016). Spatial focalization of pheromone/MAPK
711 signaling triggers commitment to cell-cell fusion. Genes Dev. *30*, 2226-2239.
712 13. Merlini, L., Khalili, B., Bendezu, F.O., Hurwitz, D., Vincenzetti, V., Vavylonis, D., and
713 Martin, S.G. (2016). Local pheromone release from dynamic polarity sites underlies cell-
714 cell pairing during yeast mating. Curr Biol. *26*, 1117-1125.
715 14. Scaduto, C.M., Kabrawala, S., Thomson, G.J., Scheving, W., Ly, A., Anderson, M.Z.,
716 Whiteway, M., and Bennett, R.J. (2017). Epigenetic control of pheromone MAPK
717 signaling determines sexual fecundity in *Candida albicans*. Proc. Natl. Acad. Sci. USA
718 *114*, 13780-13785.
719 15. Kwon-Chung, K.J. (1976). Morphogenesis of *Filobasidiella neoformans*, the sexual state
720 of *Cryptococcus neoformans*. Mycologia *68*, 821-833.
721 16. Lin, X., Hull, C.M., and Heitman, J. (2005). Sexual reproduction between partners of the
722 same mating type in *Cryptococcus neoformans*. Nature *434*, 1017-1021.
723 17. Wickes, B.L., Mayorga, M.E., Edman, U., and Edman, J.C. (1996). Dimorphism and
724 haploid fruiting in *Cryptococcus neoformans*: association with the α-mating type. Proc.
725 Natl. Acad. Sci. USA *93*, 7327-7331.

18. Fu, C., Sun, S., Billmyre, R.B., Roach, K.C., and Heitman, J. (2015). Unisexual versus bisexual mating in *Cryptococcus neoformans*: Consequences and biological impacts. Fungal Genet. Biol. *78*, 65-75.
19. Wang, L., and Lin, X. (2011). Mechanisms of unisexual mating in *Cryptococcus neoformans*. Fungal Genet. Biol. *48*, 651-660.
20. Gyawali, R., Zhao, Y., Lin, J., Fan, Y., Xu, X., Upadhyay, S., and Lin, X. (2017). Pheromone independent unisexual development in *Cryptococcus neoformans*. PLoS Genet. *13*, e1006772.
21. Xu, X., Lin, J., Zhao, Y., Kirkman, E., So, Y.S., Bahn, Y.S., and Lin, X. (2017). Glucosamine stimulates pheromone-independent dimorphic transition in *Cryptococcus neoformans* by promoting Crz1 nuclear translocation. PLoS Genet *13*, e1006982.
22. Tian, X., He, G.-J., Hu, P., Chen, L., Tao, C., Cui, Y.-L., Shen, L., Ke, W., Xu, H., Zhao, Y., et al. (2018). *Cryptococcus neoformans* sexual reproduction is controlled by a quorum sensing peptide. Nat. Microbiol. *3*, 698-707.
23. Fu, C., and Heitman, J. (2017). *PRM1* and *KAR5* function in cell-cell fusion and karyogamy to drive distinct bisexual and unisexual cycles in the *Cryptococcus* pathogenic species complex. PLoS Genet. *13*, e1007113.
24. Fu, C., Donadio, N., Cardenas, M.E., and Heitman, J. (2018). Dissecting the roles of the calcineurin pathway in unisexual reproduction, stress responses, and virulence in *Cryptococcus deneoformans*. Genetics *208*, 639-653.
25. Kwon-Chung, K.J., and Bennett, J.E. (1978). Distribution of α and **a** mating types of *Cryptococcus neoformans* among natural and clinical isolates. Am. J. Epidemiol *108*, 337-340.
26. Litvintseva, A.P., Kestenbaum, L., Vilgalys, R., and Mitchell, T.G. (2005). Comparative analysis of environmental and clinical populations of *Cryptococcus neoformans*. J. Clin. Microbiol. *43*, 556-564.
27. Cogliati, M., D'Amicis, R., Zani, A., Montagna, M.T., Caggiano, G., De Giglio, O., Balbino, S., De Donno, A., Serio, F., Susever, S., et al. (2016). Environmental distribution of *Cryptococcus neoformans* and *C. gattii* around the Mediterranean basin. FEMS Yeast Res *16*.
28. Roach, K.C., and Heitman, J. (2014). Unisexual reproduction reverses Muller's ratchet. Genetics *198*, 1059-1069.
29. Ni, M., Feretzaki, M., Li, W., Floyd-Averette, A., Mieczkowski, P., Dietrich, F.S., and Heitman, J. (2013). Unisexual and heterosexual meiotic reproduction generate aneuploidy and phenotypic diversity *de novo* in the yeast *Cryptococcus neoformans*. PLoS Biol. *11*, e1001653.
30. Saul, N., Krockenberger, M., and Carter, D. (2008). Evidence of recombination in mixed-mating-type and alpha-only populations of *Cryptococcus gattii* sourced from single eucalyptus tree hollows. Eukaryot. Cell *7*, 727-734.
31. Litvintseva, A.P., Marra, R.E., Nielsen, K., Heitman, J., Vilgalys, R., and Mitchell, T.G. (2003). Evidence of sexual recombination among *Cryptococcus neoformans* serotype A isolates in Sub-Saharan Africa. Eukaryot. Cell *2*, 1162-1168.
32. Campbell, L.T., Currie, B.J., Krockenberger, M., Malik, R., Meyer, W., Heitman, J., and Carter, D. (2005). Clonality and recombination in genetically differentiated subgroups of *Cryptococcus gattii*. Eukaryot. Cell *4*, 1403-1409.
33. Cullen, P.J., and Sprague, G.F., Jr. (2012). The regulation of filamentous growth in yeast. Genetics *190*, 23-49.

34. Phadke, S.S., Feretzaki, M., and Heitman, J. (2013). Unisexual reproduction enhances fungal competitiveness by promoting habitat exploration via hyphal growth and sporulation. Eukaryot. Cell *12*, 1155-1159.
35. Lin, X., Huang, J.C., Mitchell, T.G., and Heitman, J. (2006). Virulence attributes and hyphal growth of *C. neoformans* are quantitative traits and the *MAT*α allele enhances filamentation. PLoS Genet. *2*, e187.
36. Heitman, J., Allen, B., Alspaugh, J.A., and Kwon-Chung, K.J. (1999). On the origins of congenic MATalpha and MAT**a** strains of the pathogenic yeast *Cryptococcus neoformans*. Fungal Genet Biol *28*, 1-5.
37. Kwon-Chung, K.J. (1975). A new genus, *Filobasidiella*, the perfect state of *Cryptococcus neoformans*. Mycologia *67*, 1197-1200.
38. Kwon-Chung, K.J., Edman, J.C., and Wickes, B.L. (1992). Genetic association of mating types and virulence in *Cryptococcus neoformans*. Infect. Immun. *60*, 602-605.
39. Zhai, B., Zhu, P., Foyle, D., Upadhyay, S., Idnurm, A., and Lin, X. (2013). Congenic strains of the filamentous form of *Cryptococcus neoformans* for studies of fungal morphogenesis and virulence. Infect. Immun. *81*, 2626-2637.
40. Hsueh, Y.P., Xue, C., and Heitman, J. (2007). G protein signaling governing cell fate decisions involves opposing Gα subunits in *Cryptococcus neoformans*. Mol. Biol. Cell *18*, 3237-3249.
41. Gong, J., Grodsky, J.D., Zhang, Z., and Wang, P. (2014). A Ric8/synembryn homolog promotes Gpa1 and Gpa2 activation to respectively regulate cyclic AMP and pheromone signaling in *Cryptococcus neoformans*. Eukaryot Cell *13*, 1290-1299.
42. Feretzaki, M., and Heitman, J. (2013). Genetic circuits that govern bisexual and unisexual reproduction in *Cryptococcus neoformans*. PLoS Genet. *9*, e1003688.
43. Nielsen, K., Cox, G.M., Wang, P., Toffaletti, D.L., Perfect, J.R., and Heitman, J. (2003). Sexual cycle of *Cryptococcus neoformans* var. *grubii* and virulence of congenic **a** and α isolates. Infect. Immun. *71*, 4831-4841.
44. Huberman, L.B., and Murray, A.W. (2013). Genetically engineered transvestites reveal novel mating genes in budding yeast. Genetics *195*, 1277-1290.
45. Sprague, G.F., Jr., and Herskowitz, I. (1981). Control of yeast cell type by the mating type locus. I. Identification and control of expression of the **a**-specific gene *BAR1*. J. Mol. Biol. *153*, 305-321.
46. Banderas, A., Koltai, M., Anders, A., and Sourjik, V. (2016). Sensory input attenuation allows predictive sexual response in yeast. Nat Commun *7*, 12590.
47. Jin, M., Errede, B., Behar, M., Mather, W., Nayak, S., Hasty, J., Dohlman, H.G., and Elston, T.C. (2011). Yeast dynamically modify their environment to achieve better mating efficiency. Sci Signal *4*.
48. Shen, W.C., Davidson, R.C., Cox, G.M., and Heitman, J. (2002). Pheromones stimulate mating and differentiation via paracrine and autocrine signaling in *Cryptococcus neoformans*. Eukaryot. Cell *1*, 366-377.
49. Lin, X., Jackson, J.C., Feretzaki, M., Xue, C., and Heitman, J. (2010). Transcription factors Mat2 and Znf2 operate cellular circuits orchestrating opposite- and same-sex mating in *Cryptococcus neoformans*. PLoS Genet. *6*, e1000953.
50. Erdman, S., and Snyder, M. (2001). A filamentous growth response mediated by the yeast mating pathway. Genetics *159*, 919-928.
51. Davidson, R.C., Moore, T.D., Odom, A.R., and Heitman, J. (2000). Characterization of the MFα pheromone of the human fungal pathogen *cryptococcus neoformans*. Mol Microbiol *38*, 1017-1026.

821 52. Lang, G.I., Murray, A.W., and Botstein, D. (2009). The cost of gene expression underlies a
822 fitness trade-off in yeast. Proc. Natl. Acad. Sci. USA *106*, 5755-5760.
823 53. Tscharke, R.L., Lazera, M., Chang, Y.C., Wickes, B.L., and Kwon-Chung, K.J. (2003).
824 Haploid fruiting in *Cryptococcus neoformans* is not mating type α-specific. Fungal Genet.
825 Biol. *39*, 230-237.
826 54. Newby, G.A., and Lindquist, S. (2017). Pioneer cells established by the [*SWI*$^{+}$] prion can
827 promote dispersal and out-crossing in yeast. PLoS Biol *15*, e2003476.
828 55. Fraser, J.A., Subaran, R.L., Nichols, C.B., and Heitman, J. (2003). Recapitulation of the
829 sexual cycle of the primary fungal pathogen *Cryptococcus neoformans* var. *gattii*:
830 implications for an outbreak on Vancouver Island, Canada. Eukaryot. Cell *2*, 1036-1045.
831 56. Idnurm, A., Reedy, J.L., Nussbaum, J.C., and Heitman, J. (2004). *Cryptococcus*
832 *neoformans* virulence gene discovery through insertional mutagenesis. Eukaryot. Cell *3*,
833 420-429.
834 57. Davidson, R.C., Cruz, M.C., Sia, R.A., Allen, B., Alspaugh, J.A., and Heitman, J. (2000).
835 Gene disruption by biolistic transformation in serotype D strains of *Cryptococcus*
836 *neoformans*. Fungal Genet. Biol. *29*, 38-48.
837 58. Davidson, R.C., Blankenship, J.R., Kraus, P.R., de Jesus Berrios, M., Hull, C.M., D'Souza,
838 C., Wang, P., and Heitman, J. (2002). A PCR-based strategy to generate integrative
839 targeting alleles with large regions of homology. Microbiology *148*, 2607-2615.

840

841

Figure legends

Figure 1. Unisexual reproduction potential does not enhance competition for mating partners of the same mating type.

(A) Hyphal growth on V8 agar medium for three weeks of high (HH), intermediate (MH), low (LH), and no (NH) hyphal *MAT*α and *MAT***a** strains. The scale bar represents 500 μm. (B) Experimental design of the unisexual and bisexual mating competition. (C-E) Average cell fusion frequencies. Error bars indicate standard deviation. (C) Unisexual α-α cell fusion frequencies of high, intermediate, and low hyphal strains. (D) Bisexual **a**-α cell fusion frequencies of intermediate-high, low- intermediate, and no-low hyphal strains. (* indicates $0.01<p\leq0.05$ and ** indicates $0.001<p\leq0.01$ for each pairwise comparison) (E) Cell fusion frequencies among three *MAT*α strains of different hyphal growth phenotypes during unisexual mating competition are shown.

Figure 2. Unisexual reproduction potential enhances competition for mating partners of both mating types.

(A) **a**-α Cell fusion frequencies for mating competitions between two *MAT*α strains over a *MAT***a** strain. (B) Unisexual α-α cell fusion frequencies in the presence of *MAT***a** strains of different hyphal growth phenotypes. ** indicates $0.001<p\leq0.01$, *** indicates $0.0001<p\leq0.001$, and **** indicates $p\leq0.0001$ for each group analysis by one-way ANOVA.

Figure 3. *gpa3*Δ mutation-enhances hyphal growth and competition for mating partners of both the same and opposite mating types.

(A) Hyphal growth on V8 agar medium for one week for enhanced hyphal strain (JEC21α *gpa3*Δ::*NEO*) during unisexual (top) and unilateral bisexual (bottom) development compared to low hyphal strain (JEC21α). The scale bar represents 500 μm. (B-C) Unisexual α-α (B) and bisexual **a**-α (C) cell fusion frequencies between two low hyphal strains and between no and enhanced hyphal strains. (D-E) Cell fusion frequencies during unisexual mating competition among two low and one intermediate hyphal *MAT*α strains (D), and one low, one enhanced, and one intermediate hyphal *MAT*α strains (E). (F-G) Cell fusion frequencies during bisexual mating competition for a no hyphal *MAT***a** strain between two low hyphal *MAT*α strains (F), and between one low and one enhanced hyphal *MAT*α strain (G). (H) Unisexual α-α cell fusion frequencies between two low hyphal *MAT*α strains, and between one low and one enhanced hyphal *MAT*α strain in the presence of a no hyphal *MAT***a** strain. * indicates $0.01<p\leq0.05$ for the pairwise comparison.

Figure 4. Hyphal growth during unisexual reproduction promotes foraging for mating partners in a mating confrontation assay.

(A) Schematic diagram for the confrontation mating experiment setup. *MAT***a** cells were grown to form a line of cells, and *MAT*α cells were spot-inoculated 4

886 mm apart in parallel along the *MAT***a** cells. (B) LH, MH, HH, and EH *MAT*α
887 hyphal cells were grown towards NH, LH, and MH *MAT***a** cells for six weeks. The
888 scale bar represents 500 μm. (C) Total G418/HYG resistant colonies produced
889 by each confrontation mating pair. LH, MH, HH, and EH *MAT*α hyphal cells
890 yielded an average of 0.4, 10, 44, and 1.8 double drug resistant colonies with NH
891 *MAT***a** cells, 0.4, 26, 81, and 0.4 double drug resistant colonies with LH *MAT***a**
892 cells, 17, 239, 613, and 422 double drug resistant colonies with MH *MAT***a** cells,
893 respectively. * indicates $0.01<p\leq0.05$, ** indicates $0.001<p\leq0.01$, and ****
894 indicates $p\leq0.0001$ for each group analysis by one-way ANOVA.

895

896 **Figure 5. Pheromone response pathway activation associated with**
897 **unisexual reproduction.**

898 (A) Pheromone response pathway activation during bisexual reproduction is
899 correlated with the hyphal growth phenotype. Gene expression patterns for *MF*α,
900 *MF***a**, *STE3*α, *STE3***a**, *CPK1*, *MAT2*, *ZNF2*, and *PRM1* were examined by qRT
901 PCR (NS indicates $p\leq0.01$, * indicates $0.01<p\leq0.05$, ** indicates $0.001<p\leq0.01$,
902 *** indicates $0.0001<p\leq0.001$, and **** indicates $p\leq0.0001$ for each pairwise
903 comparison.). Crosses between MH *MAT***a** (XL280**a**) and HH *MAT*α (XL190α)
904 strains, LH *MAT***a** (XL187**a**) and MH*MAT*α (XL280α) strains, NH *MAT***a** (JEC20**a**)
905 and LH *MAT*α (JEC21α) strains, and NH *MAT***a** (JEC20**a**) and EH *MAT*α
906 (JEC21α *gpa3*Δ::*NEO*) strains were grown on V8 agar medium for 36 hours. The
907 expression levels of genes from the cross between JEC20**a** and JEC21α were
908 set to 1, and the remaining values were normalized to this. The error bars

represent the standard deviation of the mean for three biological replicates. (B) Exogenous pheromone enhances cell fusion frequency between NH *MAT***a** and LH *MAT*α strains in a dose dependent manner. p=0.0125 by one-way ANOVA. (C) EH *MAT***a** (JEC20**a** *gpa3*Δ::*ADE2 ade2*) colonies produced more hyphae in response to exogenous pheromone after three-day incubation on MS medium.

Figure 6. *gpa3*Δ mutation confers a fitness cost under mating inducing conditions.

Equal numbers of cells of (A) two low hyphal strains (JEC21α *NAT* and JEC21α *NEO*) and of (B) a low hyphal strain (JEC21α *NAT*) and an enhanced hyphal strain (JEC21α *gpa3*Δ::*NEO*) were co-cultured on YPD and V8 agar medium in the absence or the presence of equal number of cells of an intermediate hyphal **a** strain (XL280**a**). CFUs of each strain were counted before plating and after 10 days of incubation to determine competition fitness.

Figure 7. Model for the role of unisexual reproduction in foraging for mating partners.

In the absence of the opposite mating type, the ability to undergo unisexual reproduction does not promote foraging for mating partners of the same mating type (left). In the presence of the opposite mating type, hyphal growth promotes foraging for mating partners of both the same and the opposite mating type (right). NH: no hyphal growth; LH: low hyphal growth; MH: intermediate hyphal growth; HH: high hyphal growth.

931 **Supporting information**

932 **Figure S1. Derivation of the strains used in this study.**

933 B4478 *MAT*α, JEC20**a**, XL187**a**, XL190α, and XL280α are F2 progeny from the
934 cross between F1 progeny B3502 *MAT***a** and B3501 *MAT*α, which were derived
935 from a cross between the environmental isolate NIH433 *MAT***a** and the clinical
936 isolate NIH12 *MAT*α. JEC20**a** was then crossed with B4478 *MAT*α, and an α
937 progeny was backcrossed with JEC20**a**. This process was repeated 9 times to
938 yield the congenic partner B4500 JEC21α of B4476 JEC20**a**. XL280α was
939 crossed with JEC20**a**, and a *MAT***a** progeny was backcrossed with XL280α. This
940 process was repeated 9 times to yield the congenic partner XL280**a**.

941

942 **Figure S2. Hyphal growth promotes foraging for mating partners in a mini-**
943 **colony mating assay.**

944 (A) LH, MH, HH, NH, and EH *MAT*α colonies derived from single cells were
945 grown for seven days and in some cases, hyphae facilitated contact between
946 *MAT*α and *MAT***a** colonies. The scale bar represents 500 μm. (B) Cell fusion
947 frequencies between *MAT***a** and *MAT*α mating partners for each mating pair are
948 shown. * indicates $0.01<p\leq0.05$ and ** indicates $0.001<p\leq0.01$ for each group
949 analysis by one-way ANOVA.

950

951

952 **Figure S3. Pheromone response pathway activation is not correlated with**
953 **the hyphal growth phenotype.**

954 Gene expression patterns for *MF*α, *MF***a**, *STE3*α, *STE3***a**, *CPK1*, *MAT2*, *ZNF2*,
955 and *PRM1* were examined by qRT PCR (NS indicates p≤0.01, * indicates
956 0.01<*p*≤0.05, ** indicates 0.001<*p*≤0.01, *** indicates 0.0001<p≤0.001, and ****
957 indicates p≤0.0001 for each pairwise comparison.). MH *MAT***a** (XL280**a**) and HH
958 *MAT*α (XL190α) strains, LH *MAT***a** (XL187**a**) and MH*MAT*α (XL280α) strains, NH
959 *MAT***a** (JEC20**a**) and LH *MAT*α (JEC21α) strains, and an enhanced hyphal *MAT*α
960 (JEC21α *gpa3*Δ::*NEO*) strain were grown on V8 agar medium for 36 hours. The
961 expression levels of JEC20**a** or JEC21α were set to 1, and the remaining values
962 of the same mating type strains were normalized to this. The error bars represent
963 the standard deviation of the mean for three biological replicates.

964

965 **Figure S4. Exogenous pheromone has modest impact on cell-cell fusion.**

966 Cell fusion frequencies between *MAT***a** and *MAT*α cells (MH and HH, LH and
967 MH, NH and LH, and NH and EH) co-incubated on (A) V8 and (B) YPD media for
968 four days both in the absence and in the presence of 500 nM α pheromone
969 peptide.

970

971 **Figure S5. Enhanced unisexual reproduction results in a fitness cost**
972 **during vegetative growth.**

973 Hyphal growth on MS medium for two weeks for *C. neoformans* strains KN99**a**,
974 KN99**a** *gpa3*Δ::*NEO* #1, and KN99**a** *gpa3*Δ::*NEO* #2, and NH, LH, and EH *C.*
975 *deneoformans* strains JEC20**a**, JEC21α, JEC20**a** *gpa3*Δ::*ADE2 ade2*, and
976 JEC21α *gpa3*Δ::*NEO*. The scale bar represents 500 μm. Growth curves were
977 generated using an automated Tecan Sunrise absorbance reader bi-hourly for 72
978 hours.

979

980 **Figure S6. Experimental strategy for the fitness competition assay.**

981 Equal number of cells of α LH and α LH strains, and of α LH and α EH strains
982 were mixed and spot-inoculated on both YPD and V8 media both in the absence
983 and in the presence of equal number of **a** MH cells. Cells were scraped off agar
984 medium after 10 days of incubation, and both yeast cells and hyphae were
985 collected.

Table S1. Bisexual cell fusion frequencies for the mating competition experiment.

Table S2. p-Values of one-way ANOVA analyses and Welch's t-test for each pairwise comparison for the foraging for mating assay during mating confrontation.

Table S3. p-Values of one-way ANOVA analyses and Welch's t-test for each pairwise comparison for the foraging for mating assay during mating among mini-colonies.

Table S4. Strains and plasmids used in this study.

Table S5. Primers used in this study.

Table S6. Mating competition experimental design.

999 **Figure 1**

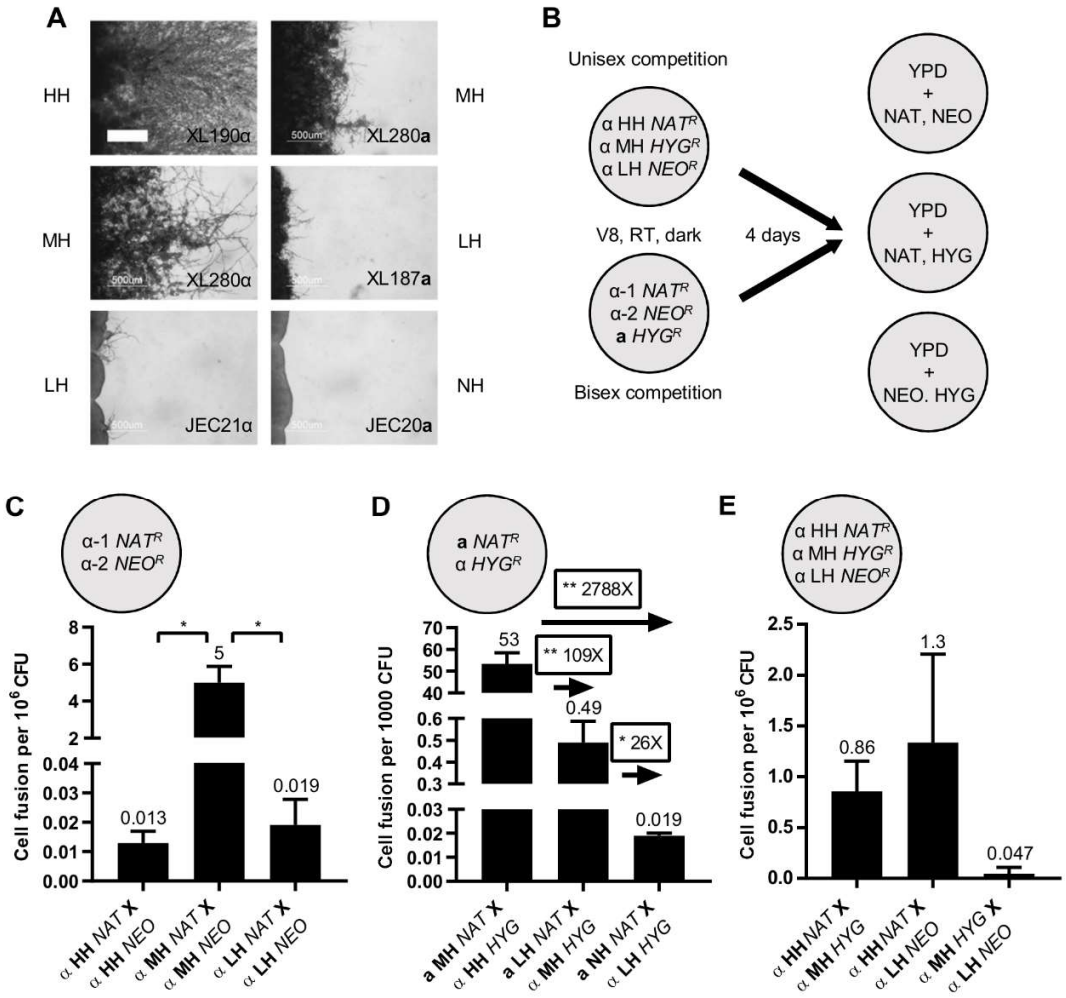

1000

1001 **Figure 2**

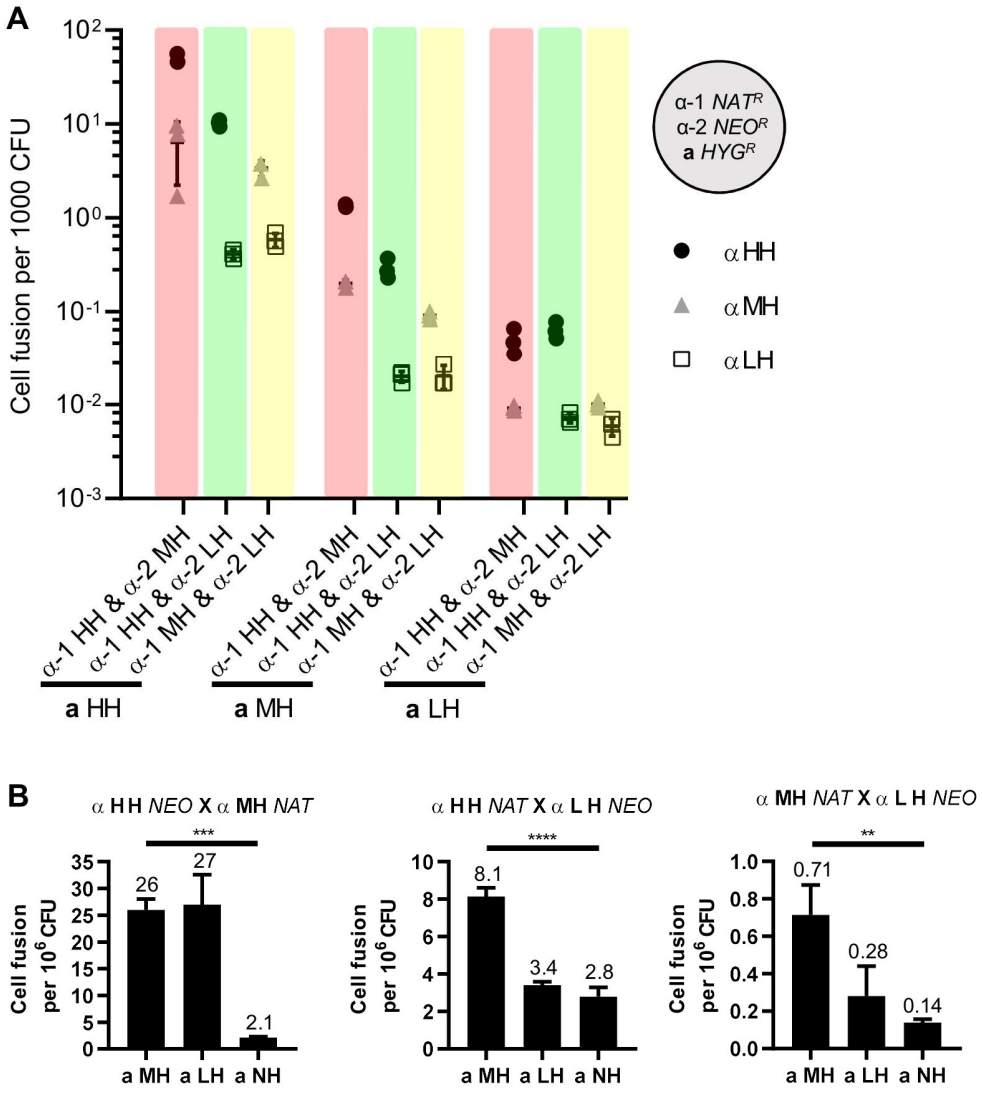

1002

1003 **Figure 3**

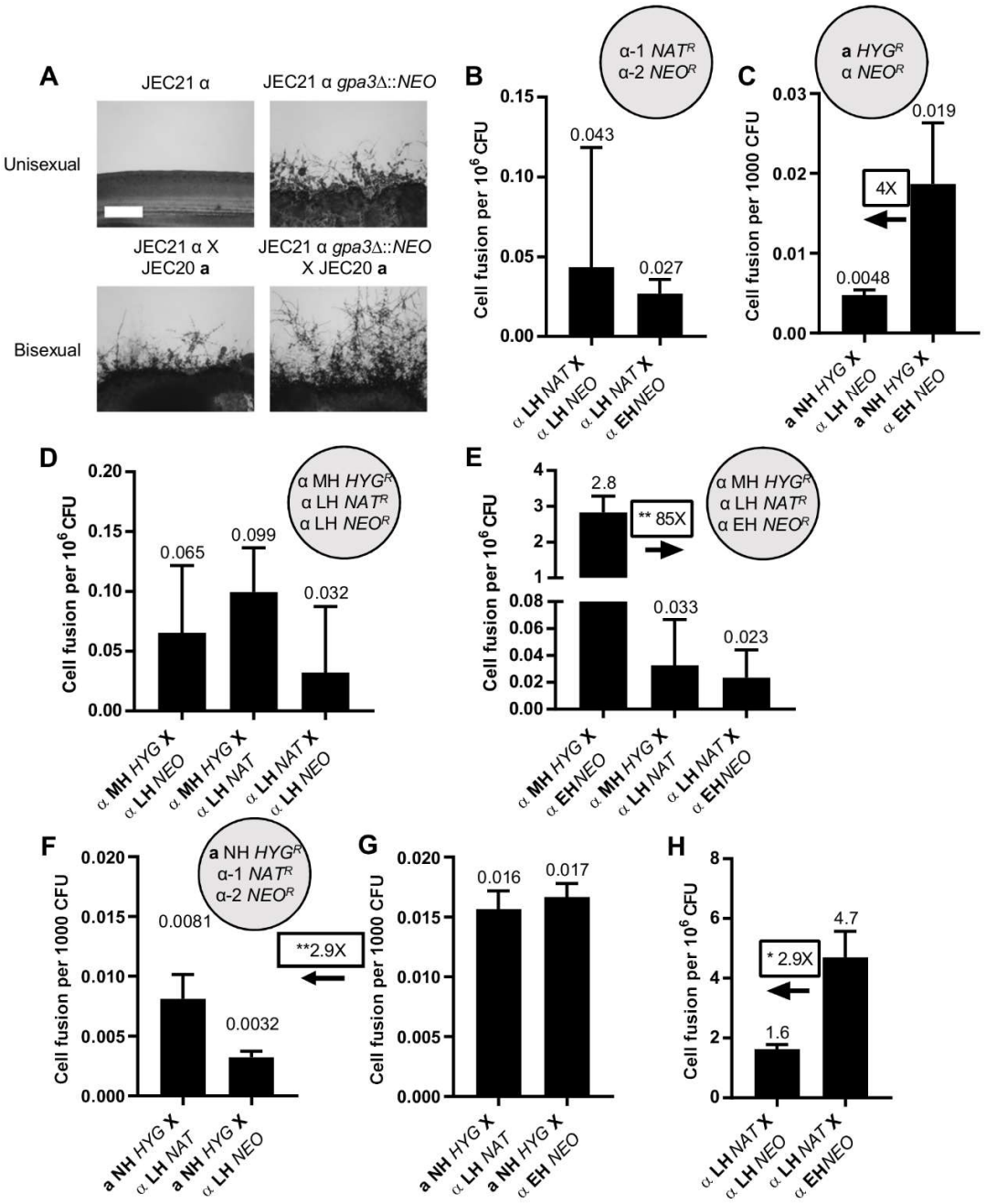

1004

1005 **Figure 4**

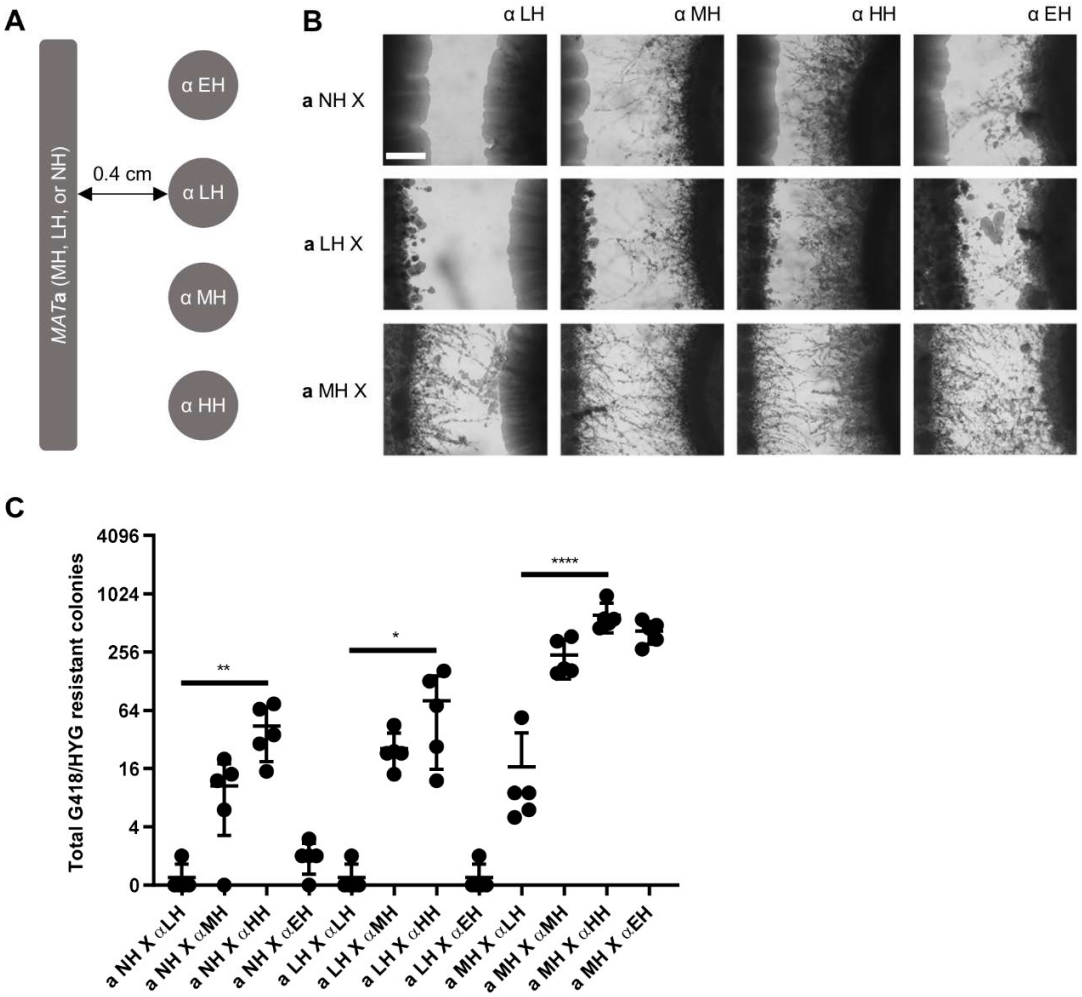

1006

1007 **Figure 5**

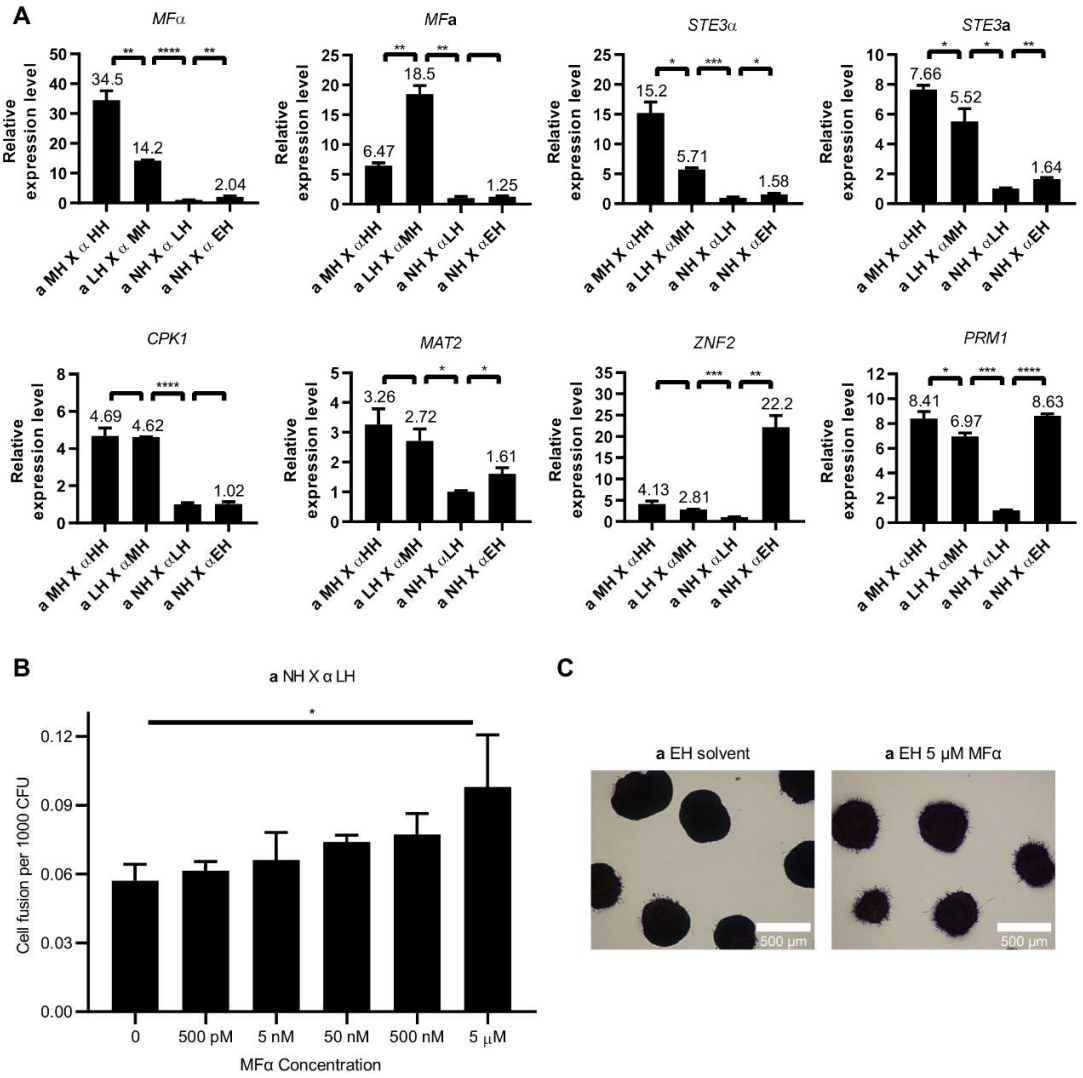

1008

1009 **Figure 6**

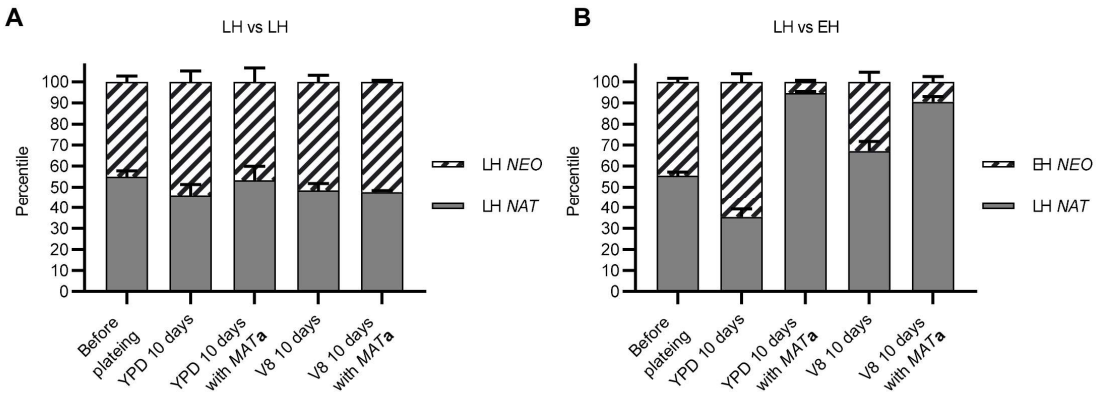

1010

1011 **Figure 7**

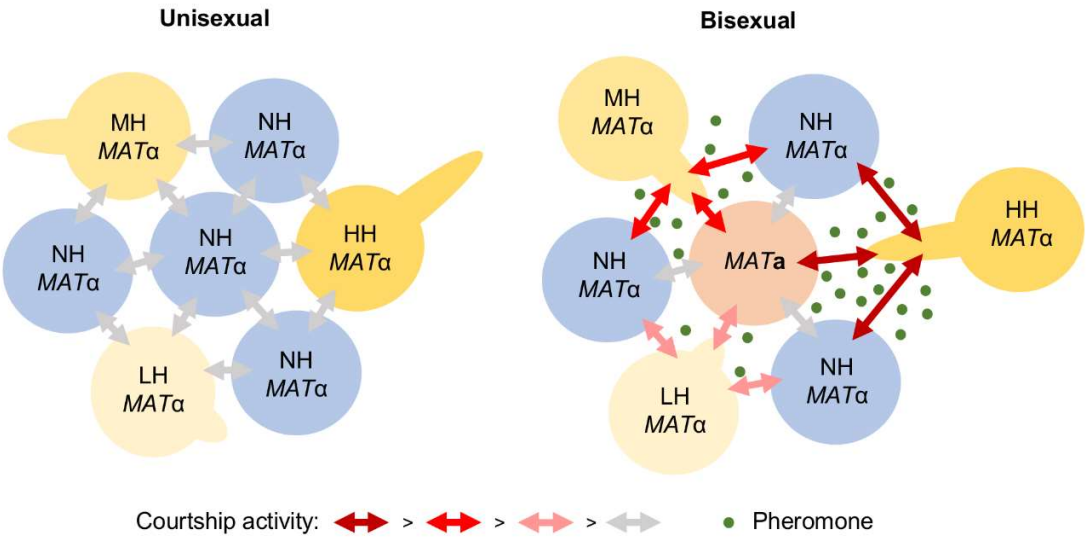

1012

1013